

# Multiple Changes of Order of the Vortex Melting Transition in $\text{Bi}_2\text{Sr}_2\text{CaCu}_2\text{O}_8$ with Dilute Columnar Defects

T. Verdene,<sup>1,\*</sup> H. Beidenkopf,<sup>1</sup> Y. Myasoedov,<sup>1</sup> H. Shtrikman,<sup>1</sup> M. Rappaport,<sup>1</sup> E. Zeldov,<sup>1</sup> and T. Tamegai<sup>2</sup>

<sup>1</sup>*Department of Condensed Matter Physics, Weizmann Institute of Science, Rehovot 76100, Israel*

<sup>2</sup>*Department of Applied Physics, The University of Tokyo, Hongo, Bunkyo-ku, Tokyo 113-8656, Japan*

(Dated: December 1, 2018)

A low concentration of columnar defects (CDs) is reported to transform a first-order vortex lattice melting line in  $\text{Bi}_2\text{Sr}_2\text{CaCu}_2\text{O}_8$  crystals into alternating segments of first- and second-order transitions separated by two critical points. As the density of CDs is increased, the critical points shift apart and the range of the intermediate second-order transition expands. A third, low temperature critical point was also observed in one sample. The measurement of equilibrium magnetization and the mapping of the melting line down to 27K was made possible by employment of the shaking technique.

PACS numbers: 74.25.Qt, 74.25.Dw, 74.72.Hs, 64.70.dg

The interplay between different energy scales of a physical system can induce phase transitions and yield a rich phase diagram. In particular, in a clean system a melting transition results from the competition between elasticity and thermal fluctuations and is usually of a first-order nature. The presence of a third competing scale due to disorder can suppress it to second order (SO) and lead to an even richer picture, the understanding of which is still quite limited [1, 2]. In order to gain insight into the various competing mechanisms, we introduce an additional control parameter in the form of a variable weak correlated disorder. We report an exceptionally intricate case, where the initially first-order (FO) melting transition of the vortex matter in a high temperature superconductor exhibits a rare three-section FO-SO-FO behavior and even seems to undergo a four-section FO-SO-FO-SO sequence. Our findings reveal that a SO transition is nucleated in a small segment along the FO transition line, bound by two critical points. This SO segment grows when the control parameter is increased thereby providing important insight into the general mechanism of transformation of a FO transition into a SO transition.

$\text{Bi}_2\text{Sr}_2\text{CaCu}_2\text{O}_8$  (BSCCO) high- $T_c$  superconductor has an especially rich vortex matter phase diagram which results from the interplay between the elasticity, thermal fluctuations, and point disorder. It consists of a FO melting line [3] which separates the low-field Bragg glass from the high-field disordered phases [4, 5, 6]. At high temperatures the FO melting transition is mainly thermally driven, whereas at lower temperatures it gradually changes its nature into a disorder-driven FO inverse melting transition [7, 8, 9]. Indications of an additional almost vertical SO glass transition line at intermediate temperatures were also found [10].

This phase diagram changes entirely with introduction of a fourth energy scale due to dense columnar defects (CDs)  $B_\phi \gg B_m(T)$ , where  $B_\phi \equiv n_{cd}\phi_0$ ,  $n_{cd}$  is the density of CDs,  $\phi_0$  is the flux quantum, and  $B_m(T)$  is the temperature-dependent melting field. Compared to

the correlated pinning energy, the elastic energy becomes negligible. As a result, the ordered solid phase is replaced by a disordered Bose glass (BoG) phase in which vortices are localized on CDs and melt through a SO BoG transition [6, 11].

In this paper we focus on the dilute CD limit, where vortices outnumber CDs at most relevant fields. Remarkably, in this limit the energy due to correlated pinning is comparable to the other three energy scales. Consequently, the four relevant energy scales mold together a particularly complex  $B - T$  phase diagram whose nature is not well-understood. Most experimental [12, 13, 14, 15, 16], theoretical [17, 18, 19] and numerical studies [20, 21, 22] agree that at high temperatures the transition remains FO. At intermediate temperatures where the melting occurs at intermediate fields  $B_m \gtrsim B_\phi$ , the pristine Bragg glass phase is replaced by a porous solid with the majority of CDs occupied by strongly pinned vortices that form an amorphous matrix. The remaining vortices form ordered crystallites that are embedded in the pores of the rigid matrix [14, 15, 16, 17, 18, 19, 20, 21, 22]. These vortex nanocrystals melt into nanodroplets apparently through a second order transition.

Experimentally, even a low density of CDs enhances hysteretic effects throughout most of the solid phase in BSCCO [12, 13]. This is a major obstacle in mapping the true thermodynamic phase transitions of vortex matter. Lacking access to the thermodynamic behavior, past experimental studies have focused on dynamics [12, 13, 14, 16, 23]. It was concluded that the high temperature FO transition line terminates at a critical point (CP) whose location depends on CD density [13, 14, 15, 16], consistent with theory and simulations [17, 18, 19, 20, 21, 22]. At temperatures below the CP, however, these out-of-equilibrium studies could not evaluate the exact nature of the transition. Thus, a SO transition was premised to exist at all temperatures below the CP [13, 14, 18, 19, 20, 21, 22], though other theoret-

ical scenarios were also considered [17]. This incomplete understanding of the dilute pinning limit led naturally to the assumption that as CD density is increased, the SO nature of melting spreads from low temperatures to higher ones with a shift of a single CP. Our findings, however, suggest an essentially different process.

Within the present study we mapped for the first time the *equilibrium* phase diagram of vortex matter with dilute CDs by performing local magnetization measurements during vortex shaking. This method [7, 10, 24, 25] utilizes an in-plane ac shaking field which agitates the vortices and assists them to assume their equilibrium positions. Tilting the magnetic field away from the CDs was shown to alter the equilibrium magnetization in YBCO crystals [26]. In contrast, in BSCCO moderate in-plane field has essentially no effect on the equilibrium properties even in presence of CDs due to the very high anisotropy [16, 27]. As a result, the ac in-plane field enhances vortex relaxation without altering the thermodynamic transitions [16]. We measured three BSCCO samples irradiated at GANIL with matching fields of  $B_\phi = 5\text{G}, 10\text{G}, 20\text{G}$  and critical temperature  $T_c \approx 92\text{K}$ , and an additional sample with  $B_\phi = 20\text{G}$  and  $T_c \approx 91\text{K}$ . Half of each sample was masked during irradiation to allow a direct comparison between pristine and irradiated behavior. The local magnetic induction of the sample was measured by an array of Hall sensors  $10 \times 10 \mu\text{m}^2$  each, while sweeping the external magnetic field  $H$  at a constant temperature. Simultaneous measurements of the transition on the pristine halves of the samples show that it remained FO throughout the temperature range. Shaking fields up to  $350\text{Oe}$  at  $10\text{Hz}$  were used.

Figure 1 presents the measured local magnetization,  $B - H$ , at (a)  $90\text{K}$ , (b)  $84\text{K}$  and (c)  $42\text{K}$ . A FO transition appears as a sharp step in  $B(H)$  and a SO transition is manifested by a break in its slope. To better resolve the nature and location of the phase transition we differentiated the measured induction  $B$  with respect to the applied field  $H$ . Figure 2 shows the derivatives  $dB/dH$  of representative (a) high temperature, (b) intermediate temperature and (c) low temperature measurements. A  $\delta$ -like peak in the derivative  $dB/dH$  indicates a FO transition, whereas a discontinuity signifies a SO transition.

At high temperatures we find that the transition remains FO in the presence of CDs, similarly to that in the pristine areas, as previously reported [13, 14]. Accordingly,  $B(H)$  in Fig. 1a shows a sharp step and the derivatives  $dB/dH$  in Fig. 2a display  $\delta$ -like peaks. At a slightly lower temperature thermal fluctuations are weaker, the effective pinning potential of the CDs gains strength and irreversibility is greatly enhanced, thus masking the underlying phase transition. We overcame this problem by applying the shaking method rendering a reversible magnetization [7, 10, 24, 25]. Figures 1b and 2b thus show equilibrium measurements at intermediate temperature

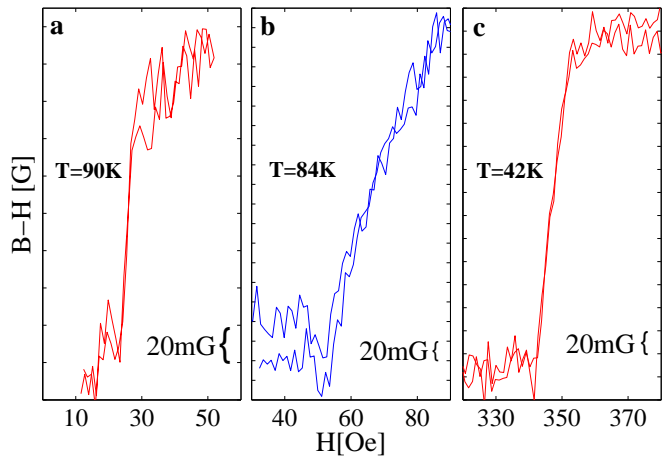


FIG. 1: (color online) The measured local magnetization,  $B - H$ , of the  $B_\phi = 10\text{G}$  sample in the presence of shaking, measured upon ascending and descending external field at constant temperatures of (a)  $90\text{K}$ , (b)  $84\text{K}$  and (c)  $42\text{K}$ . A linear slope was subtracted for clarity. The sharp steps in the local magnetization in (a) and (c) signify a FO transition. In (b), a break in the slope signifies a SO transition.

of  $B - H$  and  $dB/dH$ , respectively. A break in the slope of the induction is clearly resolved along both ascending and descending field sweeps and the derivatives display a step structure indicating a SO transition.

Yet, our main finding is the recovery of the FO thermodynamic phase transition at lower temperatures. This is clearly visible in Fig. 1c as a reversible discontinuity in magnetization  $B(H)$  and accordingly, in Fig. 2c a sharp peak in the derivatives  $dB/dH$ . This recurrence of the FO nature of the transition has been predicted theoretically [17], but has never been observed experimentally.

These findings can be explained by the following comparison of energy scales. At high temperatures thermal fluctuations are dominant enough to weaken the effective pinning potential due to CDs [13, 14, 15, 16, 17, 18, 19, 20, 21, 22, 28], resulting in a FO transition similar to that found in pristine samples. At intermediate temperatures, as correlated pinning gains dominance, the randomly distributed CDs alter the *equilibrium* vortex matter state, in addition to enhancing irreversible hysteretic behavior. At these temperatures the melting occurs at intermediate fields  $B_m \gtrsim B_\phi$  and the pristine Bragg glass phase is replaced by a porous solid with crystallites of interstitial vortices imbedded in the pores of a rigid amorphous vortex matrix [14, 15, 16]. The size of the nanocrystals within each pore is only several times their lattice constant. These dilute nanocrystals seem to melt into nanodroplets through a SO transition probably since the range of correlations is cutoff by the finite size of the pores, consistent with recent numerical simulations [19, 20, 21, 22]. This is similar to the dense CD limit, where correlated pinning dominates and vortex matter

undergoes a second order BoG transition.

At low temperatures  $\sim 40\text{K}$  the transition occurs at high fields. Each pinned vortex is surrounded by tens of interstitial vortices and the solid phase is increasingly

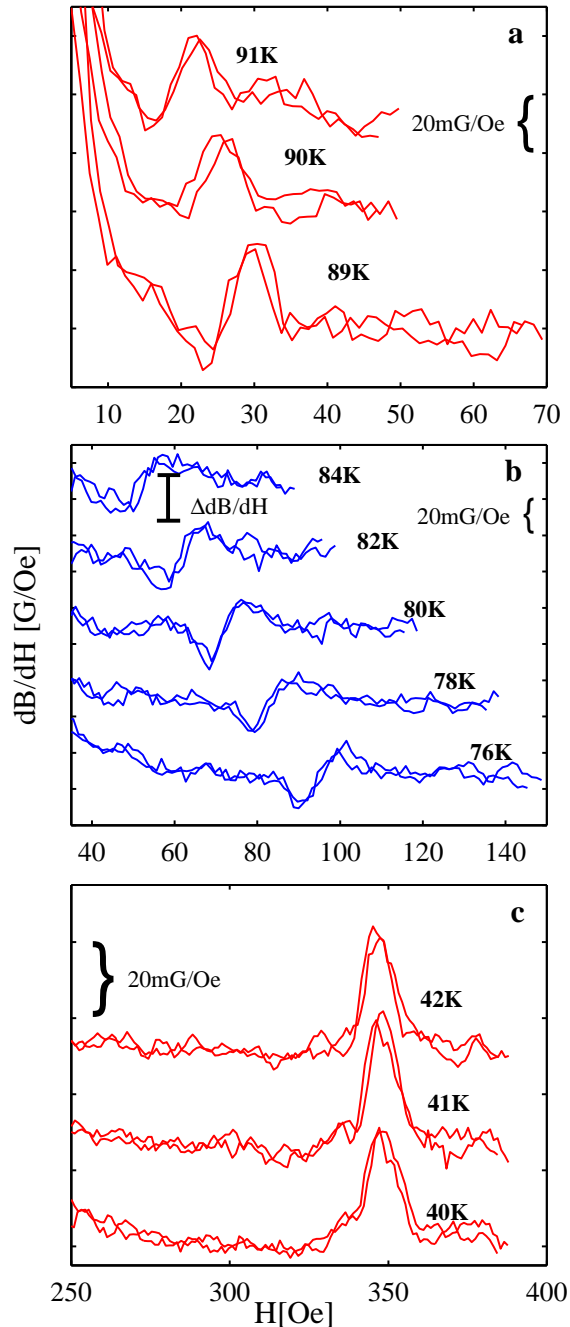


FIG. 2: (color online) The derivative of the measured induction with respect to applied field,  $dB/dH$ , of the  $B_\phi = 10\text{G}$  sample in presence of shaking, measured upon ascending and descending field at constant temperatures of (a) 89K – 91K, (b) 76K – 84K and (c) 40K – 42K. Data are shifted vertically for clarity. A peak in  $dB/dH$  in (a) and (c) signifies a FO transition, whereas a step in (b) indicates a SO transition.

dominated by inter vortex interactions [17], resulting in relatively ordered dense vortex crystallites [15]. Consequently, their melting into nanodroplets is accompanied by a discontinuity in the entropy that reflects the sharp difference in ordering of the two phases. The FO nature of the transition is thus restored, as in pristine samples.

Note that at intermediate temperatures, where the transition is SO, the step in the derivative is positive,  $\Delta\partial B/\partial H > 0$  (see Fig. 2b). This is consistent with a positive step in the specific heat,  $\Delta C_v > 0$  which was found in the high-field SO transition of pristine YBCO [29, 30]. It is in contrast, however, to the negative step of the derivative,  $\Delta\partial B/\partial T < 0$ , at the SO glass transition reported in pristine BSCCO [10]. Further study is required in order to explain the origin of these differing signs.

Interestingly, at intermediate temperatures  $dB/dH$  takes a more intricate shape; rather than a simple upward jump, it first decreases, then jumps up and finally slightly decreases again. This structure may be explained by the association of the step in the derivative at the SO transition with the relative ordering of the two phases across the transition line. Then, the decrease in the derivative might be interpreted as a slight ordering of interstitial vortices prior to the major disordering upon melting. A similar feature has been observed in the structure factors in Monte-Carlo simulations [20]. It is yet unclear, however, how these possible structural changes should affect

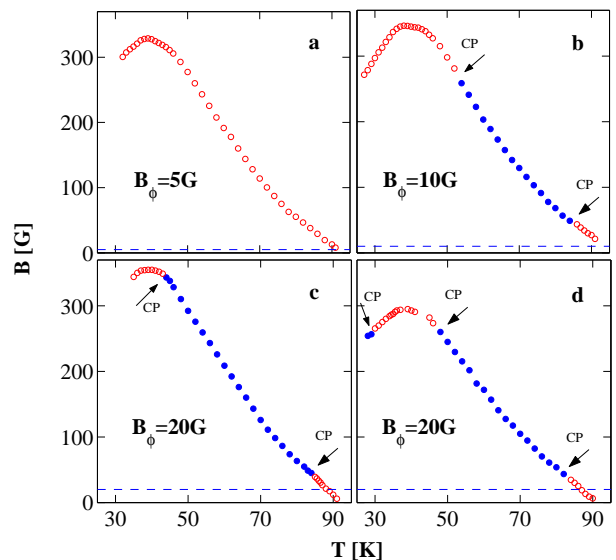


FIG. 3: (color online) Phase diagrams of irradiated BSCCO crystals showing FO ( $\circ$ ) and SO ( $\bullet$ ) transitions. (a) In  $B_\phi = 5\text{G}$  sample the transition is FO at all temperatures. (b) For  $B_\phi = 10\text{G}$  a FO-SO-FO behavior is found. (c) The SO segment expands in  $B_\phi = 20\text{G}$  sample. (d) A different  $B_\phi = 20\text{G}$  sample with lower doping that exhibits a FO-SO-FO-SO sequence. The values of  $B_\phi$  are shown by dashed lines.

the equilibrium magnetization.

The location and nature of the transition of the four samples was measured and mapped. Shaking enabled the detection of a melting transition down to 27K. The results are summarized in Fig. 3. The FO and SO regions are marked by open and solid circles respectively. In all four irradiated samples, the location of the melting line remained similar to that of the pristine parts of the samples, with a maximum at  $\sim 40$ K. The 5G sample exhibits a FO transition at all temperatures. As the density of CDs is increased, more of the  $B-T$  phase space becomes dominated by correlated disorder and consequently, a larger portion of the transition line becomes SO. The 10G and 20G samples both display two CPs with a FO-SO-FO sequence. In the 20G sample the two CPs are shifted further apart than in the 10G sample and the SO transition spreads both to high and low temperatures. We therefore suggest that this trend persists until a full SO BoG transition line is attained in the dense-pin limit.

Note that the FO transition line of irradiated samples persists to the left of its maximum in the inverse melting region (Fig. 3). These are the first equilibrium magnetization measurements in this region in presence of CDs. Figure 3d shows the phase diagram of a sample with  $B_\phi = 20$ G and a slightly lower oxygen doping. This sample displays even more intricate behavior. Like the other  $B_\phi = 20$ G and 10G samples, it also exhibits FO-SO-FO behavior. In addition, this sample reveals a third CP at extremely low temperatures on the inverse melting side of the transition. Below this CP we observe a recurrence of the SO nature of the transition. It can be attributed to the fact that the melting field decreases in the inverse melting region with decreasing  $T$ . As a result, nanocrystals contain less vortices and correlated pinning regains dominance over elasticity. Consequently, the transition becomes SO once again, similarly to that at intermediate temperatures.

It is worth pointing out the qualitative difference between the behavior reported here and the SO-FO-SO sequence found in pristine samples of the less anisotropic YBCO compound [29]. In irradiated BSCCO all three portions of the transition line separate a solid phase from a liquid phase. In pristine YBCO, however, the high-field SO portion is believed to separate two liquid phases due to the existence of a tri-critical point [30]. The low field SO portion, on the other hand, separates a solid phase from a liquid phase and is believed to arise from the intrinsic correlated disorder in YBCO crystals [31, 32].

In summary, we present thermodynamic evidence for new FO-SO-FO behavior of the melting line in BSCCO samples irradiated with a low density of CDs. This unusual behavior is due to close competition between four different energy scales in the dilute CD limit. As CDs are introduced, the melting transition initially alters its order from first to second at intermediate temperatures

where correlated pinning has a dominant effect. At high and low temperatures the transition remains FO despite the disordering potential of CDs. At low temperatures where the melting field is high, the solid phase is dominated by elasticity rather than correlated pinning due to the increasing number of vortices per CD, and the FO transition is retained. The FO nature of the transition is likewise preserved at high temperatures, where correlated pinning is weakened by thermal fluctuations. As the density of the CDs is increased, the SO segment of the transition line expands both to the higher and lower temperatures. In one sample a SO transition was also found on the low-temperature side of the inverse melting portion, resulting in an even more complex FO-SO-FO-SO sequence. The observed nucleation and growth process of the SO segments along the original FO transition line clarifies the general process of transformation of phase transitions with increased disorder. In particular, it describes the mechanism that leads to transformation of a Bragg glass in the presence of point disorder to a BoG at high concentrations of correlated disorder, which melts through a single SO transition.

We thank C.J. van der Beek and M. Konczykowski for sample irradiation and Y.Y. Goldschmidt, E.H. Brandt and G.P. Mikitik for useful discussions. This work was supported by the German Israeli Foundation (GIF), US-Israel BSF, and Grant-in-aid from the Ministry of Education, Culture, Sport, Science and Technology, Japan.

---

\* Electronic address: talhazak@wisemail.weizmann.ac.il

- [1] Y. Imry and M. Wortis, Phys. Rev. B **19**, 3580 (1979).
- [2] D.S. Fisher, M.P.A. Fisher and D.A. Huse, Phys. Rev. B **43**, 130 (1991).
- [3] E. Zeldov *et al.*, Nature **375**, 373 (1995).
- [4] T. Giamarchi and P. LeDoussal, Phys. Rev. B **52**, 1242 (1995).
- [5] T. Nattermann, Phys. Rev. Lett. **64**, 2454 (1990).
- [6] G. Blatter and V.B. Geshkenbein, *The Physics of Superconductors* (Springer, New York, 2003).
- [7] N. Avraham *et al.*, Nature **411**, 451 (2001).
- [8] G.P. Mikitik and E.H. Brandt, Phys. Rev. B **68**, 054509 (2003).
- [9] P. Olsson and S. Teitel, Phys. Rev. Lett. **87**, 137001 (2001).
- [10] H. Beidenkopf *et al.*, Phys. Rev. Lett. **95**, 257004 (2005).
- [11] D.R. Nelson and V.M. Vinokur, Phys. Rev. Lett. **68**, 2398 (1992).
- [12] M. Konczykowski *et al.*, Physica C **408**, 547 (2004).
- [13] B. Khaykovich *et al.*, Phys. Rev. B **57**, 14088 (1998); B. Khaykovich *et al.*, Physica C **282**, 2068 (1997).
- [14] S.S. Banerjee *et al.*, Phys. Rev. Lett. **90**, 087004 (2003); S.S. Banerjee *et al.*, Phys. Rev. Lett. **93**, 097002 (2004).
- [15] M. Menghini *et al.*, Phys. Rev. Lett. **90**, 147001 (2003).
- [16] N. Avraham *et al.*, Phys. Rev. Lett. **99**, 087001 (2007).
- [17] A.I. Larkin and V.M. Vinokur, Phys. Rev. Lett. **75**, 4666 (1995).

- [18] L. Radzihovsky, Phys. Rev. Lett. **74**, 4923 (1995).
- [19] J. P. Rodriguez, Phys. Rev. B **70**, 224507 (2004).
- [20] S. Tyagi and Y. Y. Goldschmidt, Phys. Rev. B **67**, 214501 (2003); Y. Y. Goldschmidt and E. Cuansing, Phys. Rev. Lett. **95**, 177004 (2005); Y. Y. Goldschmidt and Jin-Tao Liu, Phys. Rev. B **76**, 174508 (2007).
- [21] Y. Nonomura and X. Hu, Europhys. Lett. **65**, 533 (2004).
- [22] C. Dasgupta *et al.*, Phys. Rev. B **72**, 94501 (2005).
- [23] C.J. van der Beek *et al.*, Phys. Rev. Lett. **86**, 5136 (2001).
- [24] M. Willemin *et al.*, Phys. Rev. Lett. **81**, 4236 (1998).
- [25] G.P. Mikitik and E.H. Brandt, Phys. Rev. B **69**, 134521 (2004); Superconductor Science and Technology **20**, 9 (2007)
- [26] B. Hayani *et al.*, Phys. Rev. B **61**, 717 (2000).
- [27] R.J. Drost *et al.*, Phys. Rev. B **58**, 615 (1998).
- [28] S. Colson *et al.*, Phys. Rev. B **69**, 180510 (2004).
- [29] A. Schilling *et al.*, Phys. Rev. Lett. **78**, 4833 (1997).
- [30] F. Bouquet *et al.*, Nature **411**, 448 (2001).
- [31] U. Welp *et al.*, Phys. Rev. Lett. **76**, 4809 (1996).
- [32] W.K. Kwok *et al.*, Phys. Rev. Lett. **84**, 3706 (2000).